RF Performance of Large Germanium Telluride Switches for Power Application

Ismaël Charlet, Bruno Reig, Corentin Mercier, Julien Delprato, Vincent Puyal, C. Hellion, Marjolaine Allain, Stephane Monfray, Alain Fleury, Frederic Gianesello, et al.

RF Performance of Large Germanium Telluride Switches for Power Application

Ismaël Charlet[#1], Bruno Reig[#2], Corentin Mercier[$#*], Julien Delprato[#], Vincent Puyal[#], Clémence Héllion[#], Marjolaine Allain[#], Stéphane Monfray[$], Alain Fleury[$], Frédéric Gianesello[$], Philippe Cathelin[$], Jean-François Robillard[*], Emmanuel Dubois[*], Jose Lugo-Alvarez[#3]

[#]CEA-Leti, Univ. Grenoble Alpes, F-38000 Grenoble, France

[$]STMicroelectronics, 850 Rue Jean Monnet, Crolles, 38920, France

[*]University Lille, CNRS, Centrale Lille, Junia, University Polytechnique Hauts-de-France, UMR 8520 - IEMN–Institut d'Electronique de Microélectronique et de Nanotechnologie, F-59000 Lille, France

[1]ismael.charlet@cea.fr, [2]bruno.reig @cea.fr, [3]jose.lugo@cea.fr

***Abstract*— This paper reports the integration and characterization of germanium telluride (GeTe) phase-change material (PCM)-based RF switches in series configuration with a 89 µm wide PCM element to address sub-6G power handling requirements. Switching conditions using indirect heating, as well as small- and large-signal measurements are performed in this work. Devices handle power up to 37 dBm and 29 dBm respectively in ON- and OFF-state at 915 MHz. These results estimate for the first time the performances of such wide GeTe switches compatible with cellular applications and investigate technological improvement guidelines.**

***Keywords*—PCM, GeTe, phase-change RF switches, sub-6G.**

I. Introduction

The development of multiband cellphones pushes the requirements of the radio-frequency (RF) devices. In particular, RF switches set in the Frond-End Module play a key role since they route the signal to the different RF blocks and/or allow RF reconfigurability. Over the last decade, RF switches based on micromechanical system (MEMS) have been used taking benefit from good RF performance [1]-[3]. Alternatively, RFSOI switches based on PIN diodes or MOS transistors have been an industrial and mature technology for the last 10 years [4]-[6]. In this context, phase-change material (PCM) switches represent an appealing recent solution to address sub-6G and millimetre-wave applications, thanks to their low insertion loss and small footprint. They rely on the large resistance ratio between the amorphous and crystalline states of chalcogenide compounds. More precisely, germanium telluride (GeTe) is widely studied for these applications thanks to its low ON-state resistivity and large ON/OFF resistivity ratio.

Electrical switching of the PCM is achieved by applying short thermal pulses, for instance with Joule effect using micro-heaters [7]-[8]. Switches are set in OFF-state when the PCM is heated above the melting temperature and cooled quickly to quench in the amorphous state. On the opposite, the ON-state is obtained with longer thermal pulse slightly above the crystallization temperature, allowing atoms to set in the preferred crystalline state. So far, small PCM switches has been reported, with lengths and widths about 1 µm and 30 µm respectively [7]-[9]. Nevertheless, such small dimensions with reported power handling below 32 dBm will not be sufficient to handle cellular applications requiring 37 dBm.

In this work, we present the performances of GeTe based 89µm-wide and 4 µm-long RF switches. In section II, we present the switch design and fabrication. In section III, we present electrical characterization results. In section IV, we discuss the switch limitations and technological improvement guidelines. To the best of our knowledge, this is the first measurements of PCM switches with dimensions compatible with cellular applications for sub-6GHz 4G/5G FEM architectures.

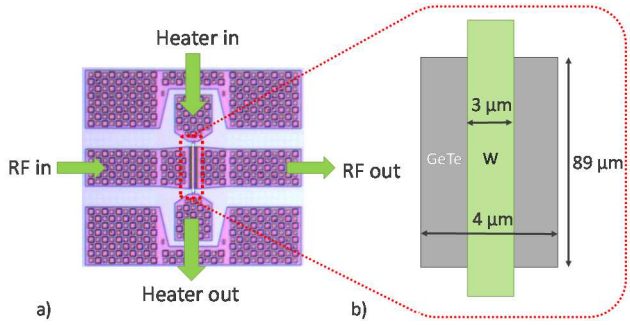

Fig. 1. (a) Optical photograph of the SPST switch (b) schematic layout of the PCM element (grey) and the heater (green).

II. PCM-Based Switch Devices and Fabrication

Using formulas presented in [10] and [11], we plotted different abacus which show that high-power cellular applications require large PCM switches. Indeed, for 37 dBm handle power and minimum FoM of 35 fs, the length must be greater than 3.5 µm and the width has to be at least 85 µm. Thus, we came up to the conclusion that a length of 4 µm was mandatory to handle 37 dBm in the OFF-state. On the other hand, to keep a reasonable R_{ON} (and thus insertion losses) a width of 89 µm has been chosen.

CPW lines are used to access the PCM element; while the material heating is achieved using a tungsten micro-heater located above the PCM (indirect heating).

The fabrication process is based on the integration of GeTe within the back-end-of-line (BEOL) of a CMOS compatible 200 mm flow. The process flow starts with a thermal oxidation of a high-resistivity (HR) silicon wafer. A first metallic layer

made of AlCu is deposited, etched and filled with silica. Next, the 100 nm-thick 0.5-0.5 GeTe is deposited and backside contacted to the underlying metal. A 100 nm-thick PVD AlN layer is deposited over the PCM as a dielectric layer, followed by a silica deposition and planarization. Heaters above the PCM are then formed, using tungsten connected to the first metallic layer. Finally, vias and the 1 µm-thick second metallic layer are formed.

III. Electrical Performances

A. Electrical Actuation

Indirect PCM switching using the heater is performed here. High speed pulses are applied between the heater electrodes using a 50 Ω-matched HP 8114A pulse generator and the resulting PCM resistance is measured with a source measurement unit (SMU) by applying a 10 mV signal.

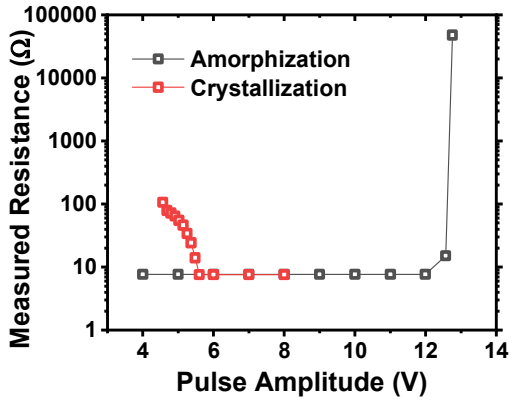

Fig. 2. Indirect switching of the SPST switch using a 400 ns long pulse for amorphization (dark) and a 1 µs long pulse for crystallization (red).

Switches are set in OFF-state by setting the PCM in the amorphous phase. To do so, the PCM must be heated above the melting temperature of 700 °C, followed by a short cooling time. Pulses used for amorphization are 400 ns wide, with 10 ns rise and fall times. Then, switches are reset in ON-state by applying a 1 µs long crystallization pulse. The pulse voltage has been swept to find the adequate conditions to achieve crystallization and amorphization and are illustrated in Fig. 2. Amorphization is achieved when a 12.7 V pulse is applied to the heater electrodes while crystallization is done for a 5.6 V pulse.

B. Small-signal Measurements

S-parameters of the RF switch have been carried out using PNAX from Keyseight. A Line-Reflect-Reflect-Match calibration is performed on a commercial Impedance Standard Substrate (ISS), using Ground-Signal-Ground (GSG) Infinity probes with a 100 µm pitch. S-parameters results are presented in Fig. 3 for the ON-state and Fig. 4 for OFF-state. A thru de-embedding is applied to extract ON-state resistance (R_{ON}) using the equation:

$$R_{ON} = 2Z_0\left(10^{(S_{thru}-S_{DUT})/20} - 1\right). \quad (1)$$

Where $Z_0 = 50\ \Omega$ is the reference impedance, S_{thru} the measured transmission of the thru de-embedding structure and S_{DUT} the switch transmission. R_{ON} is estimated about 2.5 Ω below 6 GHz (Fig. 3), corresponding to a crystal GeTe conductivity of 1.8E5 S/m which meets expectations.

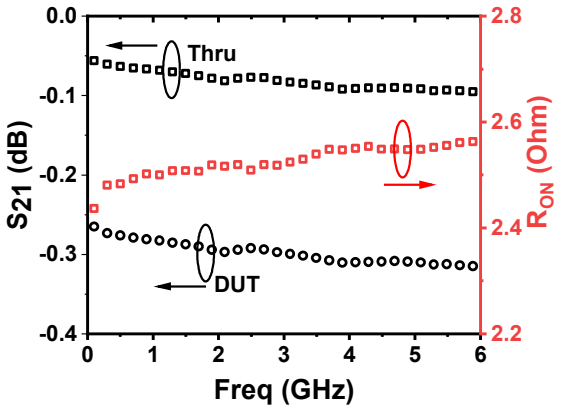

Fig. 3. Measured transmission loss of the 89 µm wide SPST in ON-state (Insertion Loss) and the thru results; with the associated R_{ON} extraction.

Next, the OFF-state capacitance (C_{OFF}) is extracted using the formula:

$$C_{OFF} = \left(4\pi f Z_0 \sqrt{10^{-S_{DUT}/10} - 1}\right)^{-1}. \quad (2)$$

Where f is the frequency, $Z_0 = 50\ \Omega$ the reference impedance and S_{DUT} the measured transmission of the SPST switch. Thus, the extracted OFF-capacitance below 6 GHz is 37.5 fF.

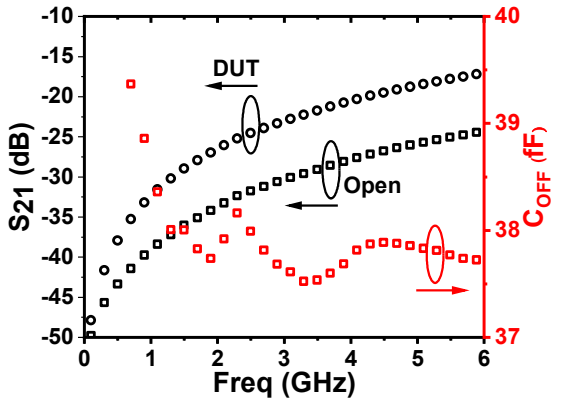

Fig. 4. Measured transmission loss of the SPST in OFF-state (Isolation) and the open structure results; with the associated C_{OFF} extraction.

C. Large-signal Measurements

Power handling is then measured at 915 MHz fundamental frequency using the bench described in Fig. 5 and calibrated with in a thru configuration. The device studied in series configuration is exposed to a power sweep from 0 dBm to 40 dBm. Fig. 6 presents the output powers for ON- and OFF-state of the 89 µm-wide switch. A 30 dBc isolation from ON-state and OFF-state is presented.

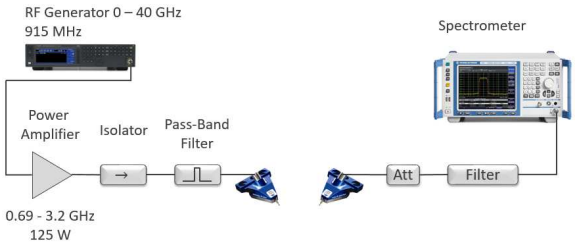

Fig. 5. Measurement setup for the power handling.

The maximal RF power before the device breakdown in the ON-state P_{RFmax}^{ON} is measured at 37 dBm which is in good agreement with expectation for such PCM dimensions. In the OFF-state, the maximal RF power before the device breakdown P_{RFmax}^{OFF} is measured at 29 dBm. This result is lower than the target since 37 dBm are expected in the OFF-state for such dimensions. This effect will be detailed in next section as well as guidelines to improve this parameter.

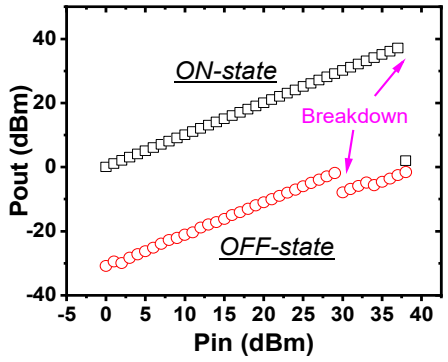

Fig. 6. Measured transmission as a function of the input power at 915 MHz for SPST in both ON and OFF states.

IV. Switch Limitations and Improvements

One well known difficult aspect of large PCM switches concerns the capability to turn "all" the material in amorphous state, since amorphization is linked to the capability to cool the material fast enough. The assumption when sizing the switch was that 2/3 of the material was amorphized, but the OFF-state power handling measurements suggest that this condition is not satisfied.

To verify this assumption we use the property that amorphization length can be accessed by fitting C_{OFF} measurements using the following equation:

$$C_{OFF} = C_{RF} + C_{GeTe} + \frac{C_H}{2} + C_F. \quad (3)$$

With C_{RF} the capacitance between the RF contacts, C_{GeTe} the capacitance between crystalline GeTe, C_H the capacitance between the crystalline GeTe and the heater and C_F the fringe capacitance, given by:

$$C_{RF} = \epsilon_0 . \epsilon_{ox} . \frac{W_{RF} . t_{cont}}{L_{RF}} \quad (4)$$

$$C_{GeTe} = \epsilon_0 . \epsilon_{GeTe} . \frac{W_{GeTe} . t_{GeTe}}{L_{RF} . \delta} \quad (5)$$

$$C_H = \epsilon_0 . \epsilon_{AlN} . \frac{W_{GeTe} . \frac{W_H - L_{RF} . \delta}{2}}{t_{DB}} . \quad (6)$$

Where W_{RF} is the PCM width here set to 89 µm, L_{RF} the RF gap set to 4 µm, t_{cont} the contact metal thickness, t_{GeTe} the GeTe thickness, ϵ_0 ϵ_{ox} ϵ_{AlN} ϵ_{GeTe} respectively the vaccum, oxide, AlN and GeTe permitivities, t_{DB} the dielectric barrier thickness, W_H the heater width set to 3 µm and δ the PCM amorphization ratio.

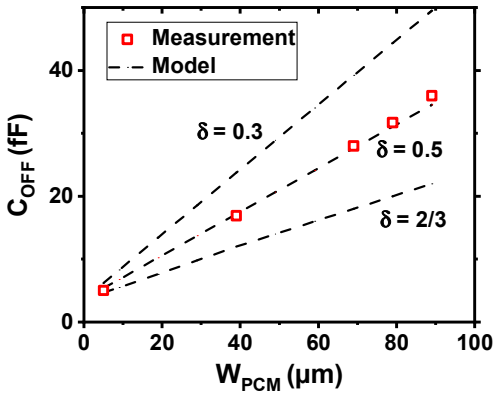

Fig. 7. Measured OFF-state capacitance of 4 µm-long switches for different widths (red) and fit curves (black) for different amorphization ratios using (3).

Herein, δ is an adjustable variable corresponding to the PCM amorphization ratio such as $\delta = 0$ means the PCM is fully cristalline while $\delta = 1$ corresponds to a fully amorphized PCM. Fig. 7 presents the C_{OFF} measurements of 4 µm long PCM with different widths and theoretical C_{OFF} from (3) for different amorphization ratios δ. This shows a clear and sensitive influence of δ on the theoretical C_{OFF}. In particular, theoretical C_{OFF} fit well with the experimental ones for $\delta = 0.5$, which is lower than the required $\delta = 2/3$ to ensure OFF-state power handling expectation. This reduced amorphization length can be explained with thermal simulations performed with COMSOL (Fig. 8).

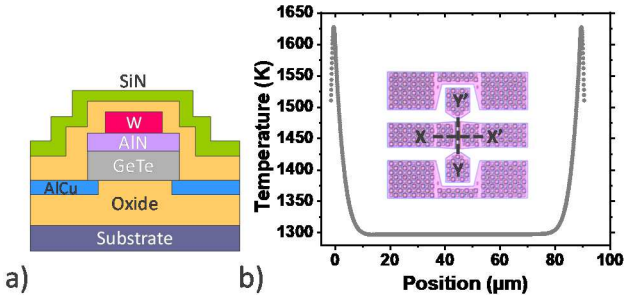

Fig. 8. COMSOL heat simulation of the studied switch (a) simulated stack cut alongside the XX'-axis (b) PCM temperature distribution alongside the YY'-axis.

The switch stack shown in Fig. 8a is simulated with an amorphization pulse sent through the heater. Fig. 8b corresponds to the resulting temperature alongside the GeTe width. This simulation shows a strong non-uniform heat profile within the PCM since temperature reaches 1300 K at the PCM

center and increases to 1630 K at the PCM edges. These heat hotspots are due to lower heat dissipation at the PCM edges. Thus, the PCM element required a longer quenching time to cool down on its edges, which ultimately degrades the amorphization process and leads to a smaller amorphization length. Besides, this non uniform temperature distribution involves a non uniform amorphization profile, which also degrades the OFF-state power handling.

An achievable area of improvement relies on the heat confinement within the heater. So far, the heater has a top encapsulation made of oxide and SiN (as in Fig. 8a) which are poor thermal conductor leading to a strong heater overheat.

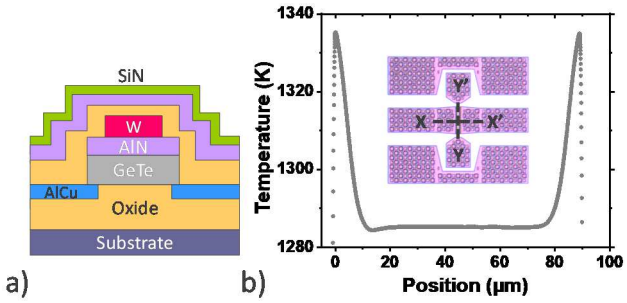

Fig. 9. COMSOL heat simulation of the studied switch with an extra AlN layer (a) simulated stack cut alongside the XX'-axis (b) PCM temperature distribution alongside the YY'-axis.

Neverthless, adding an AlN layer between the oxide and SiN top layers can help to reduce the hotpsot temperature thanks to its good heat conduction. Thermal simulations are performed for the stack of Fig. 8a but with an extra 50 nm-thick AlN layer as illustrated in Fig. 9a. The temperature alongside the PCM is shown in Fig. 9b. Here, the presence of AlN significantly lowers hotspots to 1330 K. From this, a better amorphization uniformity and a shorter quenching time can be expected, leading to a longer and more uniform amorphization area and ultimately to a better power handling in the OFF-state.

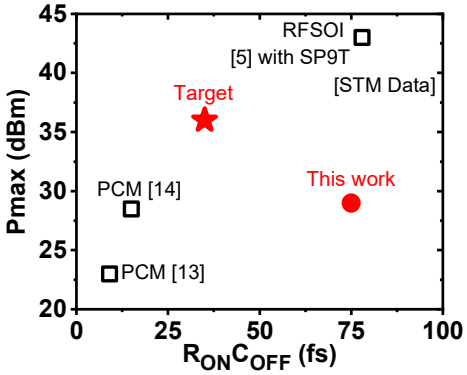

Fig. 10. Results of this work compared to state-of-the-art switches FoM and estimation for our future work with a better amorphization control. '*RFSOI [5] with SP9T*' corresponds to a SP9T device using stacked transistors of reference [5]. Measured performances of this device were shared to the authors by STMicroelectronics.

All the results present here are summarized in Fig. 10 and compared to state-of-the-art switches. In particular, reaching $R_{ON}.C_{OFF}$ = 35 fs requires a better amorphization control as explained, but also a better GeTe conductivity in the ON-state [12].

V. Conclusion

Electrical performances of GeTe-based SPST switches with dimensions compatible with cellular applications have been studied for the first time. Switches are set OFF and ON by applying a 12.7 V pulse of 400 ns and a 5.6 V pulse of 1 µs respectively. This work shows that the 89 µm wide switches can handle power up to 37 dBm at 915 MHz in the ON-state, which meets requirements for cellular applications. Besides, it is shown that future work must focus on the amorphization control. Indeed, switches handle power up to 29 dBm in the OFF-state, limited by the amorphization ratio. To reach 37 dBm in the OFF-state, mandatory for cellular applications, several guidelines are highlighted. Numerical simulations have shown that the amorphization process is degraded by hotspots at the heater edges. Thus, OFF-state power handling can be improved by reducing these hotspots, for example by adding an extra AlN layer above the heater.

References

[1] Pacheco, Sergio P., Linda PB Katehi, and CT-C. Nguyen. "Design of low actuation voltage RF MEMS switch." *2000 IEEE MTT-S International Microwave Symposium Digest (Cat. No. 00CH37017)*. Vol. 1. IEEE, 2000.

[2] Chen, Morgan Jikang, et al. "Design and development of a package using LCP for RF/microwave MEMS switches." *IEEE transactions on microwave theory and techniques* 54.11 (2006): 4009-4015.

[3] Bovadilla, R. G., et al. "Optimization of RF MEMS phase shifter for microwaves applications." *2017 32nd Symposium on Microelectronics Technology and Devices (SBMicro)*. IEEE, 2017.

[4] Foissey, O., et al. "85 fs RonxCoff and CP1dB@28GHz>25dBm Innovative PIN Diode Integrated in 55 nm BiCMOS Technology Targeting mmW 5G and 6G Front End Module." *2021 SiRF*. IEEE, 2021.

[5] Gianesello,F., et al. "Advanced 200-mm RF SOI Technology exhibiting 78 fs RON×COFF and 3.7 V breakdown voltage targeting sub 6 GHz 5G FEM." *2022 IEEE RFIC*. IEEE, 2022.

[6] https://www.skyworksinc.com/-/media/SkyWorks/Documents/Products/2201-2300/SKY13588_460LF_203512D.pdf

[7] El-Hinnawy, Nabil, et al. "A four-terminal, inline, chalcogenide phase-change RF switch using an independent resistive heater for thermal actuation." *IEEE Electron Device Letters* 34.10 (2013): 1313-1315.

[8] Borodulin, Pavel, et al. "Recent advances in fabrication and characterization of GeTe-based phase-change RF switches and MMICs." *2017 IEEE IMS*. IEEE, 2017.

[9] Singh, Tejinder, and Raafat R. Mansour. "Characterization of phase change material germanium telluride for RF switches." *2018 48th European Microwave Conference (EuMC)*. IEEE, 2018.

[10] Leon, Alexandre, et al. "RF power-handling performance for direct actuation of germanium telluride switches." *IEEE Transactions on Microwave Theory and Techniques* 68.1 (2019): 60-73.

[11] Wainstein, Nicolas, et al. "Compact modeling and electrothermal measurements of indirectly heated phase-change RF switches." *IEEE Transactions on Electron Devices* 67.11 (2020): 5182-5187.

[12] King, Matthew R., et al. "Development of cap-free sputtered GeTe films for inline phase change switch based RF circuits." *Journal of Vacuum Science & Technology B, Nanotechnology and Microelectronics: Materials, Processing, Measurement, and Phenomena* 32.4 (2014): 041204.

[13] El-Hinnawy, Nabil, et al. "Switch Stacking for OFF-State Power Handling Improvements in PCM RF Switches." *2021 IEEE IMS*. IEEE, 2021.

[14] El-Hinnawy, Nabil, et al. "Origin and optimization of RF power handling limitations in inline phase-change switches." *IEEE Transactions on Electron Devices* 64.9 (2017): 3934-3942.